Article

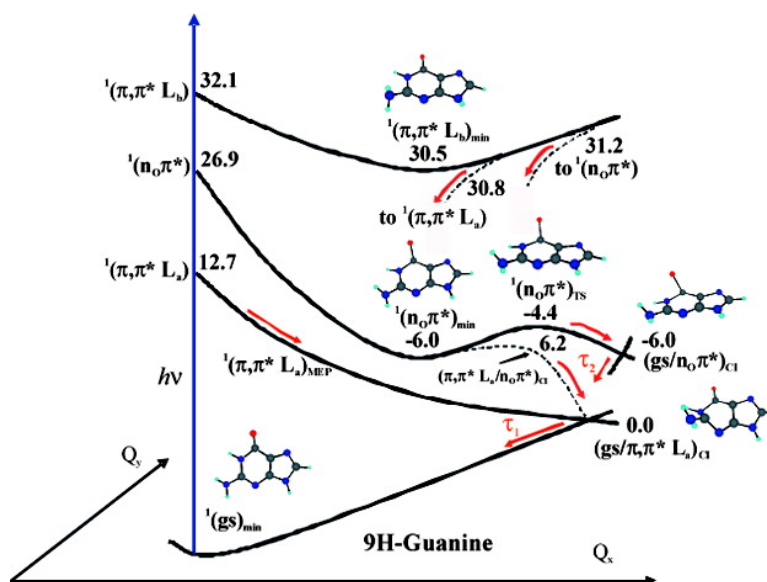# A Three-State Model for the Photophysics of Guanine

Luis Serrano-Andrs, Manuela Merchn, and Antonio Carlos Borin

More About This Article

Additional resources and features associated with this article are available within the HTML version:

- Supporting Information
- Links to the 6 articles that cite this article, as of the time of this article download
- Access to high resolution figures
- Links to articles and content related to this article
- Copyright permission to reproduce figures and/or text from this article

View the Full Text HTML

A Three-State Model for the Photophysics of Guanine

Luis Serrano-Andrés,*,† Manuela Merchán,† and Antonio Carlos Borin‡

Instituto de Ciencia Molecular, Universitat de València, Apartado 22085, ES-46071 Valencia, Spain, and Instituto de Química, Universidade de São Paulo, Av. Prof. Lineu Prestes 748, 05508-900 São Paulo, SP, Brazil

Received June 18, 2007; E-mail: Luis.Serrano@uv.es

Abstract: The nonadiabatic photochemistry of the guanine molecule (2-amino-6-oxopurine) and some of its tautomers has been studied by means of the high-level theoretical ab initio quantum chemistry methods CASSCF and CASPT2. Accurate computations, based by the first time on minimum energy reaction paths, states minima, transition states, reaction barriers, and conical intersections on the potential energy hypersurfaces of the molecules lead to interpret the photochemistry of guanine and derivatives within a three-state model. As in the other purine DNA nucleobase, adenine, the ultrafast subpicosecond fluorescence decay measured in guanine is attributed to the barrierless character of the path leading from the initially populated $^1(\pi\pi^*\ L_a)$ spectroscopic state of the molecule toward the low-lying methanamine-like conical intersection $(gs/\pi\pi^*\ L_a)_{CI}$. On the contrary, other tautomers are shown to have a reaction energy barrier along the main relaxation profile. A second, slower decay is attributed to a path involving switches toward two other states, $^1(\pi\pi^*\ L_b)$ and, in particular, $^1(n_O\pi^*)$, ultimately leading to conical intersections with the ground state. A common framework for the ultrafast relaxation of the natural nucleobases is obtained in which the predominant role of a $\pi\pi^*$-type state is confirmed.

1. Introduction

The accurate determination of the photochemistry of DNA/RNA base monomers has reached in the last few years the character of a common challenge for the communities of quantum chemical theoreticians and femtochemists. Important theoretical and experimental improvements have been achieved toward the elucidation of the photoinduced dynamics of the components of the genetic code, ready to be applied to many other systems. Since early measurements on nucleic acid base monomers in aqueous phase provided low fluorescence quantum yields[1−6] and indirect evidence of extremely efficient nonradiative decays to non-emitting states,[4−7] photostability has been established as one of the primary photophysical properties of DNA and RNA after interaction with UV light, a quality probably acquired after a long period of natural evolution.[8] Only recently has the presence of ultrafast internal conversion events in nucleic acids been directly detected in isolated conditions and condensed phases by subpicosecond techniques as an intrinsic feature of nucleotides, nucleosides, and nucleic acid base monomers.[8−12] Additional long-lived excited-state com-

ponents have been determined in polynucleotide chains and double-stranded DNA.[13−16] Time-resolved measurements on DNA/RNA nucleobases (adenine, guanine, cytosine, thymine, and uracil) seem to point out that there is a common set of mechanisms related to their internal conversion processes.[8] In particular, the most recent analysis of the data in molecular beams excited at 267 nm (4.64 eV) clearly suggests double exponential energy decays, one with a short relaxation lifetime near 100−160 fs and a second, long-lived relaxation between 0.4 and 5.1 ps.[10] The strong dependency of the conclusions on the experimental conditions and the selected exponential fits makes it difficult to obtain a clear view of the problem whose elucidation requires studies at higher resolution, solving also the role of tautomers, and a solid quantum chemical picture.

From the theoretical standpoint many efforts have been carried out trying to accurately identify favorable reaction paths and accessible decay funnels allowing efficient dissipation of the energy and ultrafast decay toward the ground state of the systems. Former proposals based on excited-state photoreactions or phototautomerisms were basically ruled out because of the

† Universitat de València.
‡ Universidade de São Paulo.
(1) Daniels, N.; Hauswirth, W. W. *Science* **1971**, *171*, 675−676.
(2) Vigny, P.; Duquesne, M. In *Organic Molecular Photophysics*; Birks, J. B., Ed.; Wiley: New York, 1977; pp 167−177.
(3) Jonas, I.; Michl, J. *J. Am. Chem. Soc.* **1978**, *100*, 6834−6838.
(4) Morgan, J. P.; Daniels, M. *Chem. Phys. Lett.* **1979**, *67*, 533−537.
(5) Callis, P. R. *Chem. Phys. Lett.* **1979**, *61*, 563−567.
(6) Callis, P. R. *Ann. Rev. Phys. Chem.* **1983**, *34*, 329−357.
(7) Peon, J.; Zewail, A. H. *Chem. Phys. Lett.* **2001**, *348*, 255−262.
(8) Crespo-Hernández, C. E.; Cohen, B.; Hare, P. M.; Kohler, B. *Chem. Rev.* **2004**, *104*, 1977−2019.
(9) Samoylova, E.; Lippert, H,: Ullrich, S.; Hertel, I. V.; Radloff, W.; Schultz, T. *J. Am. Chem. Soc.* **2004**, *127*, 1782−1786.

(10) Canuel, C.; Mons, M.; Pluzzi, F.; Tardivel, B.; Dimicoli, I.; Elhanine, M. *J. Chem. Phys.* **2005**, *122*, 074316.
(11) Pancur, T.; Schwalb, N. K.; Renth, F.; Temps, F. *Chem. Phys.* **2005**, *313*, 199−212.
(12) Kuimova, M. K.; Dyer, J.; George, M. W.; Grills, D. C.; Kelly, J. M.; Matousek, P.; Parker, A. W.; Sun, X. Z.; Towrie, M.; Whelan, A. M. *Chem. Commun.* **2005**, 1182−1184.
(13) Crespo-Hernández, C. E.; Cohen, B.; Kohler, B. *Nature* **2005**, *436*, 1141−1144.
(14) Markovitsi, D.; Onidas, D.; Gustavsson, T.; Talbot, F.; Lazzarotto, E. *J. Am. Chem. Soc.* **2005**, *127*, 17130-17131.
(15) Kwok, W. M.; Ma, C. S.; Phillips, D. L. *J. Am. Chem. Soc.* **2006**, *128*, 11894−11905.
(16) Buchvarov, I.; Wang, Q.; Raytchev, M.; Trifonov, A.; Fiebig, T. *Proc. Natl. Acad. Sci. U.S.A.* **2007**, *104*, 4794-4797.

absence of photoproducts and deuterium isotope effects in different solvents.[8] Most probably the same destiny waits for the still well-established proximity effect model, which bases the loss of emission intensity on the vibronic coupling of close-by $\pi\pi^*$ and $n\pi^*$ states, and whose limitations have been clearly demonstrated.[17] In modern photochemistry the efficiency of a radiationless decay between different electronic states taking place in internal conversion (IC) and intersystem crossing (ISC) processes is associated with the crossings of different potential energy hypersurfaces (PEHs), named conical intersections (CIs) if they take place between states of the same multiplicity, indicating explicitly the multiplicity of the states otherwise (e.g., singlet−triplet crossings). The crossings behave as funnels in whose neighborhood the transfer of population between states is highly favorable.[18,19] Locating the presence and position of the seams of CIs and, more importantly, the accessibility of such crossings by properly computing reaction energy barriers is of primary interest to determine the intrinsic decay pathways associated with base monomers. Presently, such a task cannot be accounted for without the contribution of highly accurate multiconfigurational ab initio quantum chemical methods (CASPT2 or MRCI, basically) that are able to identify decay funnels and determine accurate reaction profiles, as proved by the join efforts of different groups in recent years.[17,20−37]

Considering the great efforts performed on the other natural nucleobases,[17−29,31−35,37−41] the lack of theoretical information currently available for guanine is surprising. In fact it is the only DNA/RNA natural nucleobase in which no theoretical study has been reported in order to determine the accessibility of the nonadiabatic deactivation channels by properly computing minimum energy reaction paths. One of the reasons, apart from

its size, is undoubtedly the complex spectroscopy of the system in the gas phase, because of the known presence of several low-energy tautomers.[30] In recent years only two studies that use modern quantum chemical electronic structure methods have reported on the location of several surface crossings between low-lying states in the guanine molecule. They are the CASPT2// CASSCF study of the 9H-oxo-guanine tautomer by Chen and Li[36] and the DFT/MRCI analysis carried out by Marian[30] on several low-energy tautomers of the system, the latter focused in particular on the proper assignment of IR−UV bands in the absorption spectrum. Although relevant information was provided and several minima and CIs were located in those studies, the essential information required to properly describe the main reaction paths and rationalize the photochemistry of the system is still absent, such as the accurate calculation of the energy barriers needed to access the funnels. From the electronic structure viewpoint, only actual minimum energy path (MEP) determinations can give a proper account of the accessibility of these barriers, guaranteeing the presence or absence. It is by now well recognized that a large number of CIs can be found for multidimensional systems in regions of the PEHs with a complex structure of electronic states where degeneracy is frequent.[42,43] Multiple-state crossings take place along different paths, many of which will be totally irrelevant for the photochemistry of the system. Properly mapping the PEH implies estimating the accessibility of the CI, that is computing the energy barrier that must be surmounted to reach the funnel from the initially populated states or from state minima. Otherwise, even if the CI is located well below the energy of the initial state, it can be unimportant photochemically if a large energy barrier prevents the system from accessing such a region of the PEH. As pointed out recently by Michl,[44] most computational strategies focus on finding minimum-energy CIs (ME-CIs), which might not necessarily be the photochemically relevant structures, as it will be shown here, because the lowest-energy paths may reach the seam of CIs at higher energies, where the system will decay to the lower state. Only the computation of MEPs along relevant decay paths can properly describe the key structures.[45] This contribution includes the first report of MEPs for the photoreactivity of guanine and several of its tautomers, and complements previous studies at the CASPT2//CASSCF level of calculation of the other four nucleobases and derivatives in which MEPs have been reported for the nucleobases cytosine,[21,33] thymine,[23] uracil,[23,25] and adenine.[17,24,34]

The focus of this paper will be placed on the accurate determination of the relevant lowest-energy photochemical reaction channels in the four most stable tautomers of the guanine molecule (see Figure 1), and in particular in the biologically relevant 1H-9H-2-amino-6-oxopurine (hereafter 9H-guanine) tautomer. Computation of excitation energies, oscillator strengths, minimum energy paths, CIs, seam of CIs, transition states, and samples of classical trajectory simulations performed at the ab initio CASPT2//CASSCF level of calculation, will lead

(17) Serrano-Andrés, L.; Merchán, M,; Borin, A. C. *Proc. Natl. Acad. Sci. U.S.A.* **2006**, 8691−8696.
(18) Olivucci, M., Ed. *Computational Photochemistry*; Elsevier: Amsterdam, 2005.
(19) Domcke W., Yarkony D. R., Köppel, H., Eds. *Conical Intersections*; World Scientific: Singapore, 2004.
(20) Merchán, M.; Serrano-Andrés, L. *J. Am. Chem. Soc.* **2003**, *125*, 8108−8109.
(21) Merchán, M.; Serrano-Andrés, L.; Robb, M. A.; Blancafort, L. *J. Am. Chem. Soc.* **2005**, *127*, 1820−1825.
(22) Serrano-Andrés, L.; Merchán, M.; Lindh, R. *J. Chem. Phys.* **2005**, *122*, 104107.
(23) Merchán, M.; González-Luque, R.; Climent, T.; Serrano-Andrés, L.; Rodríguez, E.; Reguero, M.; Peláez, D. *J. Phys. Chem. B* **2006**, *110*, 26471−26476.
(24) Serrano-Andrés, L.; Merchán, M.; Borin, A. C. *Chem. Eur. J.* **2006**, *12*, 6559−6571.
(25) Climent, T.; González-Luque, R.; Merchán, M.; Serrano-Andrés, L. *Chem. Phys. Lett.* **2007**, *441*, 327−331.
(26) Matsika, S. *J. Phys. Chem. A* **2004**, *108*, 7584−7590.
(27) Kistler, K. A.; Matsika, S. *J. Phys. Chem. A* **2007**, *111*, 2650−2661.
(28) Marian, C. M. *J. Chem. Phys.* **2005**, *122*, 104314.
(29) Tomic, K.; Tatchen, J.; Marian, C. M. *J. Phys. Chem. A* **2005**, *109*, 8410−8418.
(30) Marian, C. M. *J. Phys. Chem. A* **2007**, *111*, 1545−1553.
(31) Perun, S.; Sobolewski, A. L.; Domcke, W. *J. Am. Chem. Soc.* **2005**, *127*, 6257−6265.
(32) Perun, S.; Sobolewski, A. L.; Domcke, W. *J. Phys. Chem. A* **2006**, *110*, 13238−13244.
(33) Blancafort, L.; Cohen, B.; Hare, P. M.; Kohler, B.; Robb, M. A. *J. Phys. Chem. A* **2005**, *109*, 4431−4436.
(34) Blancafort, L. *J. Am. Chem. Soc.* **2006**, *128*, 210−219.
(35) Chen, H.; Li, S. H. *J. Phys. Chem. A* **2005**, *109*, 8443−8446.
(36) Chen, H.; Li, S. H. *J. Chem. Phys.* **2006**, *124*, 154315.
(37) Nielsen, S. B.; Sølling, T. I. *ChemPhysChem* **2005**, *6*, 1276−1281.
(38) Gustavsson, T.; Banyasz, A.; Lazzarotto, E.; Markovitsi, D.; Scalamani, G.; Frisch, M. J.; Barone, V.; Improta, R. *J. Am. Chem. Soc.* **2006**, *128*, 607−619.
(39) Zgierski, M. Z.; Patchkovskii, S.; Lim, E. C. *J. Chem. Phys.* **2005**, *123*, 081101.
(40) Zgierski, M. Z.; Patchkovskii, S.; Fujiwara, T.; Lim, E. C. *J. Phys. Chem. A* **2005**, *109*, 9384−9387.
(41) Zgierski, M. Z.; Patchkovskii, S.; Lim, E. C. *Can. J. Chem.* **2007**, *85*, 124−134.

(42) Truhlar, D. G.; Mead, C. A. *Phys. Rev. A* **2004**, *68*, 032501.
(43) Dreuw, A.; Worth, G. A.; Cederbaum, L. S.; Head-Gordon, M. *J. Phys. Chem. B* **2004**, *108*, 19049−19055.
(44) Michl, J. In *Computational Photochemistry*; Olivucci, M., Ed.; Elsevier: Amsterdam, 2005.
(45) Serrano-Andrés, L.; Merchán, M. In *Photostability and Photoreactivity in Biomolecules: Quantum Chemistry of Nucleic Acid Base Monomers and Dimers*; Leszczynski, J., Shukla, M., Eds.; Springer: New York, 2007.
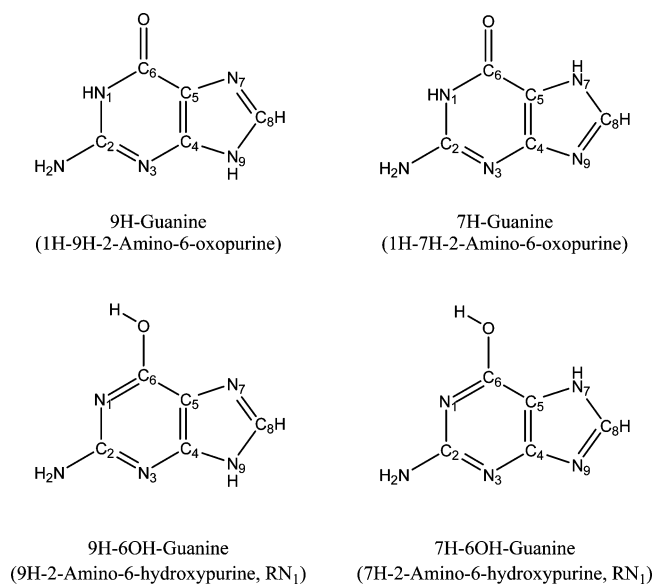
Figure 1. Structure and labeling of the studied guanine tautomers. The names given in this contribution and the IUPAC names (within parentheses) are included. RN_1 is the cis rotamer (toward N_1).

us to propose a three-state model for the photochemistry of guanine, similar to that already successfully found for adenine in our previous studies.[17,24] We shall also emphasize the importance of the so-called photochemical reaction path approach,[46] the theoretical strategy based on mapping the minimum energy path for the efficient transit of the energy in the excited states toward accessible CIs. Such a procedure and the use of highly accurate quantum chemical methods will certainly provide the key parameters to understand most photochemical mechanisms and will constitute the basis for future theoretical studies on the dynamics of the system which may lead to ultimately predict the time evolution of the process. Our complete set of calculations on the nucleobases will allow us to design a global and common model to rationalize the photochemistry of the five natural nucleobases.[23,45]

2. Methods and Computational Details

Optimizations of minima, transition states (TS), potential energy hypersurface (PEH) crossings, and minimum energy paths (MEPs) have been here performed initially at the CASSCF level of theory for the studied tautomers of guanine. MEPs have been built as steepest descent paths in which each step requires the minimization of the PEH on a hyperspherical cross section of the PEH centered on the initial geometry and characterized by a predefined radius (see Supporting Information).[47] At the computed geometries, CASPT2 calculations[48,49] on several singlet states were carried out in order to include the necessary dynamic correlation effects. The protocol is usually named CASPT2//CASSCF and has proved its accuracy repeatedly.[17,45,50−54]

In some cases, at the obtained CASSCF crossings, CASPT2 explorations at close geometries were performed in order to find lowest-energy CASPT2 crossings, related to CIs, at the highest level of calculation. The one-electron atomic basis set 6-31G(d,p) was used throughout for energy optimizations and energy differences in order to obtain a balanced description of the PEH. The minor influence of diffuse functions to describe low-lying valence excited states of similar molecules was shown previously.[55] Studies of low-lying Rydberg states have been in any case reported.[30] The accuracy of the present strategy can be compared to our previous study on guanine in which large ANO-type basis sets and diffuse functions were employed.[56] To check the precision of the calculations, results obtained with an ANO-S C,N,O [3s2p1d]/H [2s1p] basis set will be also discussed. Structure optimizations and MEPs for $\pi\pi^*$-type states used initially a π active space of 12 electrons and 10 orbitals (the lowest nodeless π orbital was kept inactive), whereas two lone-pair in-plane orbitals were added for $n\pi^*$ states. The active spaces were extended with additional extra-valence orbitals in control calculations to account for the reliability of the results. Unless otherwise specified (see also Supporting Information), the final CASSCF/CASPT2 results use an active space of 14 electrons distributed in 12 orbitals, which include all $\pi\pi^*$ orbitals except the lowest in energy plus two lone-pair orbitals, and seven state-average roots. No symmetry restrictions were imposed during the calculations that employed in most cases the *MOLCAS-6* set of programs.[57] From the calculated CASSCF transition dipole moments (TDM) and the CASPT2 band origin energies, the radiative lifetimes have been estimated by using the Strickler−Berg relationship.[53,58,59] Nonadiabatic coupling CASSCF elements were obtained with the *Gaussian 03* program.[60] Additional technical details can be found in the Supporting Information.

3. Results and Discussion

3.1 Structure of Excited States in Guanine. The guanine molecule is essentially a derivative of a purine ring in which one amine and one carbonyl group have been added in position C_2 and C_6, respectively (see Figure 1). Adenine, in the meanwhile, is a 6-aminopurine. A similar structure of low-lying excited states can be expected in purine and in the related nucleic acid bases. In particular, CASPT2 calculations for the 9H-purine tautomer placed at the Franck−Condon (FC) ground-state optimized geometry, the low-lying $\pi\pi^*$ singlet excited states at 4.66 eV ($\pi\pi^*$ L_b) and 5.09 eV ($\pi\pi^*$ L_a), whereas for the 7H-tautomer the states were obtained reversed at 4.68 eV ($\pi\pi^*$ L_a) and 5.17 eV ($\pi\pi^*$ L_b). In both cases an $n_N\pi^*$ singlet state was found lower in energy at 3.76 and 2.87 eV, respectively.[61] We have employed the usual Platt−Murrell's nomenclature[62,63] in which, in terms of the CASSCF natural orbitals (NOs), the L_a label represents the state with a large contribution to the CASSCF wave function of the electronic configuration HOMO (H) → LUMO (L), whereas L_b involves a multiconfigurational

(46) Bernardi, F.; Olivucci, M.; Robb, M. A. *Pure Appl. Chem.* **1995**, *67*, 17−24.
(47) De Vico, L.; Olivucci, M.; Lindh, R. *J. Chem. Theory Comput.* **2005**, *1*, 1029−1037.
(48) Andersson, K.; Malmqvist, P.-Å., Roos, B. O. *J. Chem. Phys.* **1992**, *96*, 1218−1226.
(49) Finley, J.; Malmqvist, P.-Å.; Roos, B. O.; Serrano-Andrés, L. *Chem. Phys. Lett.* **1998**, *288*, 299−306.
(50) Serrano-Andrés, L.; Merchán, M.; Nebot-Gil, I.; Lindh, R.; Roos, B. O. *J. Chem. Phys.* **1993**, *98*, 3151−3162.
(51) Roos, B. O.; Andersson, K.; Fülscher, M. P.; Malmqvist, P.-Å.; Serrano-Andrés, L.; Pierloot, K.; Merchán, M. *Adv. Chem. Phys.* **1996**, *93*, 219−331.
(52) Merchán, M.; Serrano-Andrés, L. In *Computational Photochemistry*; Olivucci, M., Ed.; Elsevier: Amsterdam, 2005.

(53) Serrano-Andrés, L.; Merchán, M. In *Encyclopedia of Computational Chemistry*; Schleyer, P. v. R., Schreiner, P. R., Schaefer, H. F., III, Jorgensen, W. L., Thiel, W., Glen, R. C., Eds.; Wiley: Chichester, 2004.
(54) Serrano-Andrés, L.; Merchán, M. *J. Mol. Struct. (THEOCHEM)* **2005**, *729*, 109−118.
(55) Jean, J. M.; Hall, K. B. *J. Phys. Chem. A* **2000**, *104*, 1930−1937.
(56) Fülscher, M. P.; Serrano-Andrés, L.; Roos, B. O. *J. Am. Chem. Soc.* **1997**, *119*, 6168−6176.
(57) Andersson, K.; et al. *MOLCAS*, version 6.4; Department of Theoretical Chemistry, Chemical Centre, University of Lund, Lund: Sweden, 2006.
(58) Strickler, S. J.; Berg, R. A. *J. Chem. Phys.* **1962**, *37*, 814−822.
(59) Rubio-Pons, O.; Serrano-Andrés, L.; Merchán, M. *J. Phys. Chem. A* **2001**, *105*, 9664−9676.
(60) Frisch, M. J.; et al. *Gaussian 03*; Gaussian Inc.: Wallingford CT, 2004.
(61) Borin, A. C.; Serrano-Andrés, L.; Fülscher, M. P.; Roos, B. O. *J. Phys. Chem. A* **1999**, *103*, 1838−1845.
(62) Platt, J. R. *J. Chem. Phys.* **1949**, *17*, 484−495.
(63) Murrell, J. N. *The Theory of the Electronic Spectra of Organic Molecules*; Chapman and Hall: London, 1971.

Table 1. Computed Spectroscopic Properties for the Low-Lying Singlet Excited States of the Most Stable Tautomers of Guanine at the CASPT2//CASSCF Level of Calculation[a]

	absorption			emission			
states	VA	f	μ/D	T_e	VE	τ_{rad}	(gs/$\pi\pi$*)$_{CI}$
9H-Guanine (9H,1H-2-amino-6-oxopurine)[b]							
^{1}(gs)			5.81				
^{1}($\pi\pi$* L$_a$)	4.93	0.158	5.23				4.3[c]
^{1}(n$_O\pi$*)	5.54	0.002	3.51	4.56	2.7	553	
^{1}($\pi\pi$* L$_b$)	5.77	0.145	4.92	5.69	4.6	5	
7H-Guanine (7H,1H-2-amino-6-oxopurine)							
^{1}(gs)			2.26				
^{1}($\pi\pi$* L$_a$)	5.08	0.137	4.14	4.51	3.8	9	(3.6)[c]
^{1}(n$_O\pi$*)	5.33	0.002	5.49	4.31	2.5	990	
^{1}($\pi\pi$* L$_b$)	5.39	0.121	1.65	5.04	4.4	8	
9H-6OH-Guanine (9H-2-amino-6-hydroxypurine)							
^{1}(gs)			2.90				
^{1}($\pi\pi$* L$_b$)	4.95	0.033	3.24	4.52	3.2	37	
^{1}(n$_N\pi$*)	5.34	0.006	4.78	d	—	—	
^{1}($\pi\pi$* L$_a$)	5.67	0.271	3.49	5.14	4.4	4	(4.2)[c]
7H-6OH-Guanine (7H-2-amino-6-hydroxypurine)							
^{1}(gs)			4.20				
^{1}($\pi\pi$* L$_a$)	4.79	0.058	3.19	4.26	4.0	24	(3.9)[c]
^{1}(n$_N\pi$*)	5.02	0.006	2.99	4.29	3.0	244	
^{1}($\pi\pi$* L$_b$)	5.71	0.023	4.58	5.17	4.0	41	

[a] VA: vertical absorption, VE: vertical emission. T_e: band origin. Energies in eV, lifetimes (τ_{rad}) in ns. [b] The ^{1}(n$_N\pi$*) state was placed vertically at 6.60 eV in a previous study.[56] [c] Adiabatic energy difference for (gs/$\pi\pi$*)$_{CI}$. In 9H-guanine ^{1}($\pi\pi$* L$_a$) has no minimum along the MEP, and the CI is reached in a barrierless way from FC. In the other systems the CI was obtained as a minimum energy CI (MECI). See text. [d] The optimization leads directly to a conical intersection with the ground state, (gs/n$_N\pi$*)$_{CI}$, at 4.12 eV.

description including especially the H → L + 1 and H − 1 → L configurations. The presence of the substituents on the six-membered ring slightly changes the excited state structure. In adenine, in which simply a NH$_2$ group has been added to C$_6$, both 9H and 7H tautomers keep the order ^{1}L$_b$ and ^{1}L$_a$, yielding CASPT2 excitation energies 5.16 and 5.35 eV (9H), and 5.06 and 5.41 eV (7H), respectively, with the transition to the ^{1}L$_a$ state carrying most of the intensity.[17,24] Changes in guanine are expected to be larger, because the changes involve carbonylic substitution on C$_6$ (changing therefore the π ring structure, see Figure 1) and amino substitution on C$_2$. Table 1 compiles the present CASPT2 calculations on the excited-state structure and properties for the four guanine tautomers studied here, which have been determined as the most stable forms in the gas phase.[30] Regarding the 9H- and 7H-guanine tautomers, they both have a similar sequence of states at 4.93 and 5.77 eV (9H) and 5.08 and 5.39 eV (7H) keeping the order ^{1}L$_a$ and ^{1}L$_b$, respectively, precisely opposite to those of adenine[17,24] and 9H-purine.[61]

For the case of guanine, transitions to both $\pi\pi$* states carry similar intensities. If we focus first on the reason for the changes, the HOMO-like orbital in guanine (its structure is similar for purine and adenine, see Supporting Information) has a large bonding character between C$_2$ and N$_3$, and therefore, any substitution on those atoms will strongly affect the position of the ^{1}L$_a$ state. In guanine, for instance, as in 2-aminopurine,[17] the H → L ^{1}L$_a$ state is clearly stabilized from that in purine to be the lowest-lying singlet excited state, unlike what happens in adenine, in which position C$_2$ is not substituted and the ^{1}L$_a$ state remains high in energy as the third singlet state at the FC region.[17,24]

Regarding the hydroxyl tautomers of guanine, the change of the π structure of the six-membered ring implies a modification of the character of the states at the FC region, although the obtained energies are similar. For the 9H-6OH-guanine tautomer, the low-lying state is of ^{1}L$_b$ character at 4.95 eV, whereas the ^{1}L$_a$ state is computed at 5.67 eV and carries most of the population on absorption, features which can be found similar in adenine. For 7H-6OH-guanine the ^{1}L$_a$ state is however stabilized upon substitution on position N$_7$. As can be expected, the character of the low-lying nπ* states changes from the oxo- to the hydroxypurines, from involving the oxygen (n$_O\pi$*) to the nitrogen (n$_N\pi$*) σ in-plane electronic lone pairs, that in all cases relate to essentially forbidden transitions. Although the *trans*- or *anti*-(RN$_7$) conformation of 9H-6OH-guanine has been found to be as stable as the *cis*- or *syn*-(RN$_1$) rotamer in previous theoretical calculations,[30,64,65] we have selected for our study the latter structures in the hydroxyl tautomers. In view of the previous results on 7H-adenine, they could be considered less prone to give rise to stable planar structures by forming intramolecular hydrogen bonds, becoming therefore better candidates to decay directly toward an out-of-plane CI. Apart from the theoretical consensus obtained in that the 7H-guanine tautomer is the most stable form in the gas phase, it can be also assumed that all four tautomers computed here (*cf.* Figure 1) plus the 9H-6OH-guanine RN$_7$ rotamer have relative stabilities so similar that the five should be present to some extent in the molecular beams.[30]

One of the most intense debates in the photophysics of guanine has been focused on the proper assignment of the IR−UV bands in the gas phase to the different tautomers (see ref 30 and references therein). As such an aspect has been carefully discussed previously and it is not the goal of the present research, we can just mention that the present results agree with most of the previous conclusions, in particular with the aspect more relevant to understand the photochemistry of the system. The band origin corresponding to the lowest-energy singlet excited state of the biologically active tautomer, 9H-guanine, is absent from the resonant two-photon ionization spectra. The reason for the absence is related to the existence of an easily accessible CI along the relaxation path of the ^{1}($\pi\pi$* L$_a$) state of 9H-guanine, a unique feature of the natural tautomer not present in the other forms. That implies the lack of stationary minimum along the barrierless MEP leading from the FC region to a CI with the ground state (see Table 1 and section 3.2.). The presence of such a favorable relaxation path is consistent with the detected ultrafast decay of the energy in guanine samples, and therefore with the proposed absence of IR−UV absorption peaks for this tautomer. Interestingly the 7H-guanine has been discarded[30,66] as a source of the band origin peaks in the UV spectrum because it was supposed to decay extremely fast from the S$_1$ state, like 9H-guanine. We report here, however, a high-lying planar minimum found for the former along the MEP on ^{1}($\pi\pi$* L$_a$) that is a plausible candidate to be assigned to the resolved peaks in the spectrum. Our current hypothesis is that the ultrafast decay in 7H-guanine is not as favorable as that in 9H-guanine because of the presence of such local minimum along the main relaxation path. Also, it must be

(64) Gorb, L.; Kaczmarek, A.; Gorb, A.; Sadlej, A. J.; Leszczynski, J. *J. Phys. Chem. B* **2005**, *109*, 13770−13776.
(65) Shukla, M. K.; Leszczynski, J. *Chem. Phys. Lett.* **2006**, *429*, 261−265.
(66) Chen, H.; Li, S. H. *J. Phys. Chem. A* **2006**, *110*, 12360−12362.

pointed out that the assignment of T_e band origins on the basis of computed adiabatic transition requires the use of a more accurate basis set than 6-31G(d,p). Control calculations performed with the ANO-S basis set (see section 2) indicate that excitation energies for the $\pi\pi^*$ states typically decrease by nearly 0.2−0.3 eV.[56] As proved before,[17,24] such differences have no consequence regarding the photochemical discussion in the present research.

3.2. Photoinduced Reactivity in DNA/RNA Nucleobases: A Qualitative View. By inspection of the molecular structure of guanine (9H and 7H) it is possible to predict the most relevant degrees of freedom that may be activated, upon UV light absorption. The basic features are the same as those already known in the photochemistry of heteroaromatic rings, closely related to the paths followed by ethene and substituted ethenes after light irradiation.[67] Ethene relaxes its low-lying $\pi\pi^*$ excited-state by undergoing a combination of stretching/twisting deformations of the double bond combined with pyramidalization of the terminal hydrogens. As proved some time ago,[68] the larger is the difference in electronegativities between the two atoms forming the double bond, the smaller is the $S_0−S_1$ gap upon 90° twisting, and therefore smaller should be the pyramidalization or equivalent distortion requested to yield a degeneracy. In a ring, double bond torsions and pyramidalizations are constrained, and the deformation yields out-of-plane ring puckering. In the six-membered ring of the pyrimidine nucleobases we find one double carbon−carbon ethylenic bond C_5C_6 (C_4C_5 in purines), plus one carbon−nitrogen double bond C_4N_3 (single or double C_6N_1 bond in purines) in cytosine. One (two in cytosine) ethene (CC)- or methanamine (CN)-like CI can therefore be expected between the lowest-lying S_0 and S_1 states after distortion of the double bond, and they have been described in the literature as (gs/$\pi\pi^*$)-like (C_4C_5 hereafter) and (gs/$n\pi^*$)-like (C_6N_1 hereafter).[20,23,25−29,33,39,45,67,69] It can be observed that the CC-like (gs/$\pi\pi^*$) CI in the three molecules, uracil, thymine, and cytosine, gives rise to a more strongly distorted structure than the CN-like CI,[20,27] as corresponding to a distortion of an apolar C=C bond. Following the recent work by Barbatti and Lischka[67] and using Boeyens nomenclature for puckered six-membered rings (see Figure SI1 in the Supporting Information for definitions),[67,70,71] we can describe the CC-like CI as having almost a screw-boat (S) conformation $^5S_6$, whereas the CN-like CI in cytosine resembles an envelope structure ^3E, with one single atom out of the ring plane.

As shown previously,[17,24] and also in the present paper, purine nucleobases, apart from the C=N bond of the five-membered ring, have two C_2N_3 and C_4C_5 double bonds, whereas an additional C_6N_1 bond is present in the adenine six-membered ring (also in 6OH-guanines). The inter-ring C_4C_5 bond is strongly strained and larger in purines than in pyrimidines (e.g., 1.342 Å in uracil[25] and 1.369 Å in guanine); therefore, it cannot play the same role as in the one-ring nucleobases. The C_2N_3 bond will be therefore a common protagonist of the photochemistry of purines, giving rise to a low-lying S_0/S_1 metha-

namine CN-like CI in both adenine and guanine, as it has been certainly obtained in quantum chemical calculations relating the lowest-lying singlet $\pi\pi^*$ states.[17,24,28,32,34−36,45] Deformations taking place in the six-membered ring correspond to an envelope structure ^2E, in which the C_2 atom lies out-of-plane with respect to the other five atoms. In adenine, another CI is found, here with (gs/$n_N\pi^*$) character, by stretching/twisting of the C_2N_3 bond plus ring puckering, giving rise to another envelope conformation, ^6E.[17,24] As will be shown below, this qualitative view becomes at the end more complex, for instance when a (gs/$n_O\pi^*$) low-lying CI is also found involving rotation of the guanine C_6N_1 bond and strong ring puckering, ^6E, or when considering CI obtained by in-plane C=O stretching, as in cytosine.[20,21] Regarding the five-membered ring, its corresponding distortions can be expected at higher energies and include ring-opening at the puckered site.[67] Under the conditions of most of the experiments performed, for instance irradiation at 267 nm (4.64 eV), the most significantly populated state is the H → L $^1(\pi\pi^*$ $L_a)$ singlet state in adenine, whereas the lower $^1(\pi\pi^*$ $L_b)$ state will be populated through the ^1L_a state decay. In guanine, where the $^1(\pi\pi^*$ $L_b)$ is higher in energy, both states seem to be populated similarly at high energies (see also oscillator strengths in Table 1), consistent with experimental findings in solvent phases.[72] Upon H → L $\pi\pi^*$ excitation only the C_2N_3 and C_4C_5 bonds can be expected to be weakened (the H and L molecular orbitals have bonding and antibonding character in those bonds, respectively, see Supporting Information) and to be the protagonists of the low-energy photochemistry. The activation of C_4C_5 in purines is, however, unlikely at low energies because of the restriction imposed by the five-membered ring, therefore leaving C_2N_3 as the common bond for low-energy photoactivated distortion. In the next section we will show how actual calculations relate with these qualitative expectations.

3.3. Nonadiabatic Photochemistry of the Biological Tautomer 9H-Guanine. By using sophisticated quantum chemical algorithms for searching surface crossings we can locate a number of CIs along the PEH of a molecule, in particular the most relevant ones between the S_0 and S_1 states, required to explain ultrafast dissipation of the energy after UV absorption. Even when such structures can be characterized with great precision, they may easily become irrelevant for the photochemistry of the system if the energy barrier to access them is too large. As mentioned in the introduction, the photochemical path approach, that is computing minimum energy paths from the initially populated states, seems the most reliable strategy to determine the key question in nonadiabatic photochemistry: Is the crossing seam accessible? Figure 2 displays the CASPT2// CASSCF MEP computed along the lowest-lying $^1(\pi\pi^*$ $L_a)$ H → L state of the 9H-guanine molecule. Starting at the FC geometry, the MEP leads freely and in a barrierless way toward a CI with the ground state, (gs/$\pi\pi^*$ $L_a)_{CI}$, in which the stretching/ twisting of the C_2N_3 bond brings the molecule to adopt an acute ^2E envelope puckered structure on the six-membered ring. As seen in Table 1 the CI is computed at 4.3 eV adiabatically from the ground-state minimum, and it has been located by a specific CI search starting from the geometry of the crossing provided by the MEP, which turned out to be identical in practice to the

(67) Barbatti, M.; Lischka, H. *J. Phys. Chem. A* **2007**, *111*, 2852−2858.
(68) Bonačiæ-Kouteck×c6, V.; Kouteck×c6, J.; Michl, J. *Angew. Chem., Int. Ed. Engl.* **1987**, *26*, 170−189.
(69) Ismail, N.; Blancafort, L.; Olivucci, M.; Kohler, B.; Robb, M. A. *J. Am. Chem. Soc.* **2002**, *124*, 6818−6819.
(70) Boeyens, J. C. A. *J. Cryst. Mol. Struct.* **1978**, *8*, 317−320.
(71) Evans, D. G.; Boeyens, J. C. A. *Acta Crystallogr., Sect. B* **1989**, *45*, 581−590.

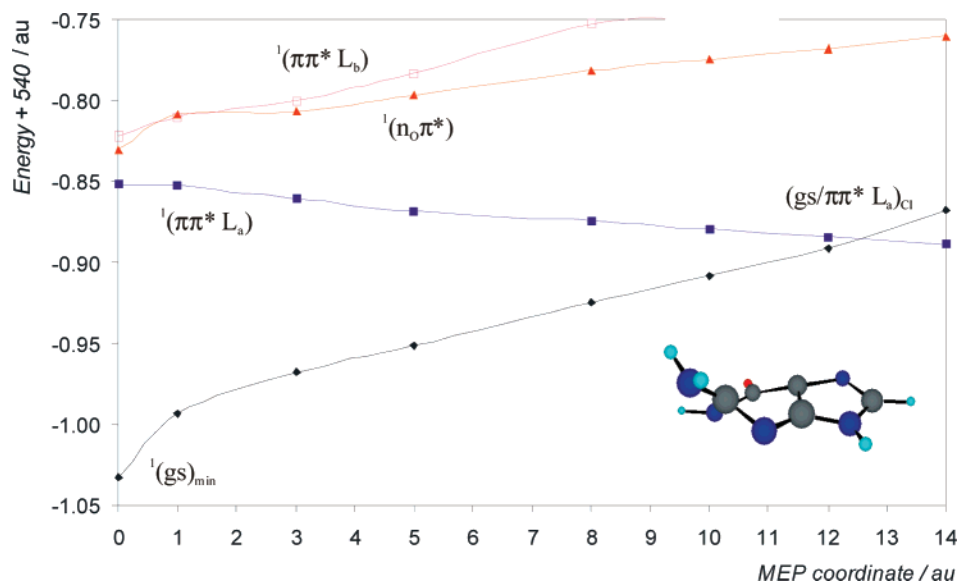(72) Cohen, B.; Crespo-Hernández, C. E.; Kohler, B. *Faraday Discuss.* **2004**, *127*, 137−147.

Figure 2. Low-lying singlet excited states of 9H-guanine computed at the CASPT2//CASSCF level from the Franck−Condon ground-state geometry along the minimum energy path (MEP) on the $^1(\pi\pi^* L_a)$ state. $(gs/\pi\pi^* L_a)_{CI}$ lies at 4.3 eV adiabatically from the ground-state minimum.
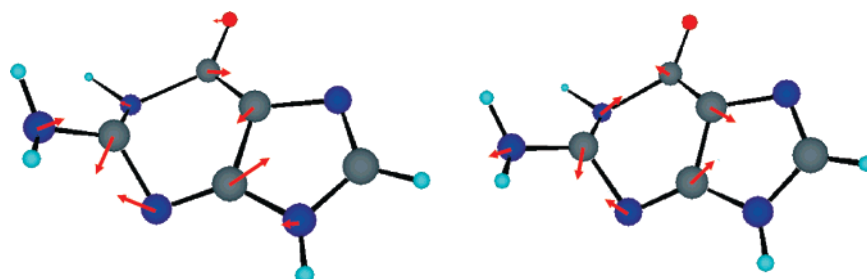

Figure 3. Branching vectors x_1 (energy difference gradient, left) and x_2 (coupling vector, right) for the minimum energy conical intersection $(gs/\pi\pi^* L_a)_{CI}$ in 9H-guanine. Arrows represent dominant motions expressed in atom-centered Cartesian coordinates.

finally obtained $(gs/\pi\pi^* L_a)_{CI}$ structure. An important point should therefore be highlighted. We do not find any stationary minimum along the MEP, and our suggestion is that the most favorable relaxation path is totally barrierless, unlike previous proposals that placed a minimum along the decay profile.[36] As regards the characterization of the CI, the calculation of the tuning and coupling vectors, x_1 and x_2, both displayed in Figure 3, provides relevant information about the efficiency of a CI to promote nonadiabatic transitions.

Both vectors define the branching plane where the degeneracy of the states is lifted linearly. In this case, the x_2 derivative coupling vector points toward a restoration of the planarity of the ring and the amino group, whereas the x_1 gradient difference vector increases the pyramidalization in C_2 and, as it will be shown below, relates to a minimum energy structure found along the seam of CIs. From the viewpoint of the electronic structure, the molecule at the seam has a biradical character, with pronounced electron localization on the C_2 and C_5 atoms, as observed in the CASSCF H and L molecular orbitals (MOs) obtained at the CI geometry (see Figure 4), which also indicate some delocalization on $C_5C_4N_3$. Those MOs contribute predominantly to the description of both ground and $^1(\pi\pi^* L_a)$ states in the region of the crossing seam.

According to the present results, the internal conversion between the $^1(\pi\pi^* L_a)$ and the ground states is predicted to be extremely favorable. The barrierless character of the reaction path perfectly relates to the femtosecond (148 fs) decay
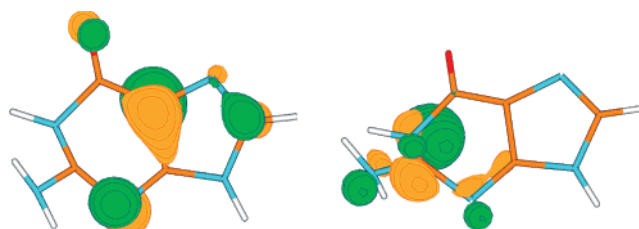

Figure 4. Structure of the HOMO-like (left) and LUMO-like (right) natural orbitals (NOs) in the CASSCF wave function of 9H-guanine at the conical intersection $(gs/\pi\pi^* L_a)_{CI}$. Both NOs are the main contributors to the biradical character of the system, centered at C_5 and C_2.

measured in the time-resolved experiments of molecular beams of guanine.[10] It is important to point out that the computation of a MEP has many advantages in comparison to other theoretical strategies such as, for instance, the calculation of minimum energy CIs (MECIs). In an independent calculation, a MECI involving similar deformations as that CI located close to the end of the MEP (although smaller ring ^2E puckering) was identified at 4.1 eV adiabatically from the ground-state minimum. The MECI structure is similar to that reported previously.[30] The two CIs, that near the end of the MEP (4.3 eV) and the MECI (4.1 eV), are separated by an energy barrier. Even if they participate in the same seam of CIs, they do not belong to the same relaxation path, as we will show below. If we focus on the process without excess energy, from the initially populated state, $^1(\pi\pi^* L_a)$, the energy will tend to follow the steepest descent path along the MEP, and it will be transferred
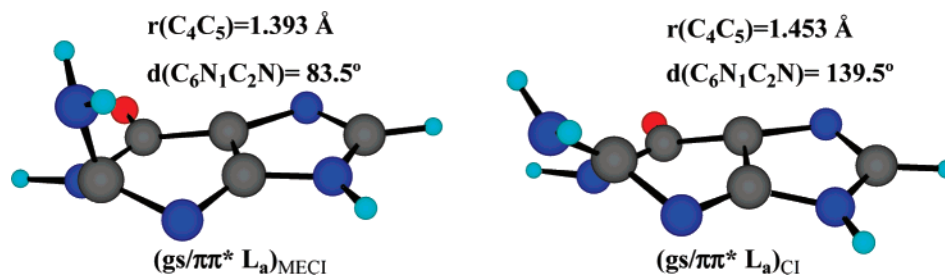
r(C$_4$C$_5$)=1.393 Å

d(C$_6$N$_1$C$_2$N)= 83.5°

(gs/$\pi\pi$* L$_a$)$_{MECI}$

r(C$_4$C$_5$)=1.453 Å

d(C$_6$N$_1$C$_2$N)= 139.5°

(gs/$\pi\pi$* L$_a$)$_{CI}$

Figure 5. Structures and key parameters of different conical intersections of the same seam in 9H-guanine, optimized as a minimum energy conical intersection (MECI) ((gs/$\pi\pi$* L$_a$)$_{MECI}$, left, 4.1 eV adiabatically) and with a CI search at the end of the minimum energy path (MEP) along the ^{1}($\pi\pi$* L$_a$) state ((gs/$\pi\pi$* L$_a$)$_{CI}$, right, 4.3 eV adiabatically).
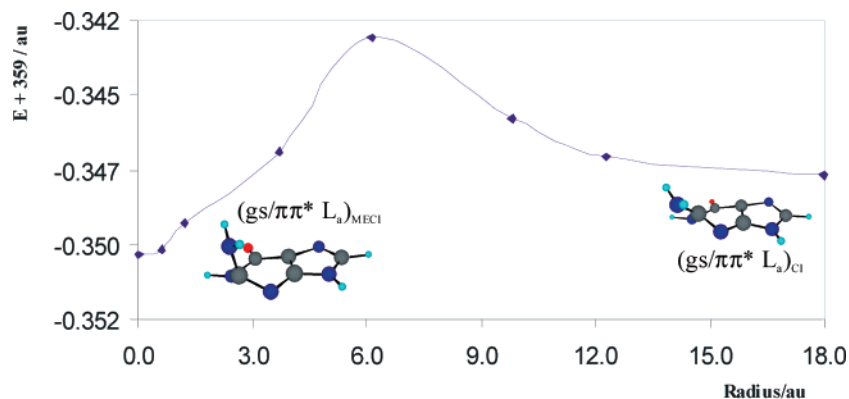

Figure 6. Computed CASSCF path for the seam of degeneracy points (gs/$\pi\pi$* L$_a$) in 9H-guanine from the minimum energy conical intersection (MECI), left at radius 0.0 au, toward the crossing at the end of the minimum energy path (MEP), right at radius 18.0 au. Simultaneous constraints including degeneracy in the energy and addition of the radius of the hypersphere have been used at each point.

to the lower state in its first approach to the seam of CIs, in this case close to the end of the MEP (see Figure 2). It is unlikely that the system has to ride the seam toward the MECI. The distinct structures can be observed in Figure 5. We have highlighted the two most important internal coordinates: on going from the end of the MEP (photochemically the most relevant structure) to the MECI, the C$_4$C$_5$ bond length enlarges nearly 0.06 Å, and the dihedral angle C$_6$N$_1$C$_2$N increases 56°. Hereafter, both structures will be labeled (gs/$\pi\pi$* L$_a$)$_{CI}$, for the CI close to the end of the MEP, and (gs/$\pi\pi$* L$_a$)$_{MECI}$, for that obtained as the lowest-energy CI. The former, (gs/$\pi\pi$* L$_a$)$_{CI}$, shall be considered the photochemically relevant structure.

In order to analyze this important question we have performed calculations along the seam connecting our computed (gs/$\pi\pi$* L$_a$)$_{MECI}$ and (gs/$\pi\pi$* L$_a$)$_{CI}$ (see Figure 5). The two CIs belong to the same seam, which can be followed by including additional constraints to the searching algorithm (that is, apart from imposing the degeneracy condition, a path can be built by forcing the solution to remain within the predefined radius of a hypersphere) as it is performed to compute MEPs. In Figure 6 we have included a profile computed along the seam of (gs/$\pi\pi$* L$_a$) CIs performed with the mentioned strategy. Starting at the (gs/$\pi\pi$* L$_a$)$_{MECI}$ structure (radius 0.0 au), the various points of the seam can be obtained by using different constrained radii. The (gs/$\pi\pi$* L$_a$)$_{CI}$, at the end of the computed seam and also close to the end of the MEP (Figure 6, right), is higher in energy than the computed (gs/$\pi\pi$* L$_a$)$_{MECI}$ (left); however, the former is the relevant funnel for the photochemistry, considering that it is the easiest way in which the system can decay to the ground state. The energy barrier found along the path from that structure to the MECI would have to be surmounted in order to

decrease the pyramidalization of C$_2$ and place the amino group perpendicular to the ring. It is important to notice that such a barrier is photochemically irrelevant, because the system will never ride the seam; it will just decay immediately after reaching the first funnel, (gs/$\pi\pi$* L$_a$)$_{CI}$, at the end of the MEP. This was not the case, for instance in the secondary relaxation path in adenine,[17,24] where the profile connecting the n$_N\pi$* minimum to the (gs/n$_N\pi$*)$_{CI}$ contained a transition state in which a few kcal mol^{-1} energy barrier was computed, representing the same type of distortion in NH$_2$. In that case, as such a barrier does not belong to the seam of CIs, it becomes photochemically relevant. In any case, it has to be pointed out that a detailed characterization of the seam requires the use of second-derivative techniques.[73,74]

As listed in Table 1, the third ^{1}($\pi\pi$* L$_b$) singlet excited-state in 9H-guanine has also a noticeable, related oscillator strength, 0.145. We have computed the MEP along the ^{1}($\pi\pi$* L$_b$) state starting at the FC geometry, and it is displayed in Figure 7. After crossing the n$_O\pi$* state, the MEP reaches a planar minimum, except for the hydrogen atoms of the amine group, in the ^{1}($\pi\pi$* L$_b$) state, as it happened in the case of adenine.[17,24] It is therefore unlikely that the state is directly involved in any of the ultrafast relaxation processes, and just when populated at high energies it may decay toward any of the low-lying states, such as ^{1}($\pi\pi$* L$_a$) or ^{1}(n$_O\pi$*) through respective CIs. We have computed a number of singular points related with the three low-lying singlet excited states of 9H-guanine, in particular, states minima, transition states, and several CIs, and the results are summarized in Table 2 (see also Supporting Information).

(73) Yarkony, D. R. *J. Chem. Phys.* **2005**, *123*, 204101.
(74) Sicilia, F.; Blancafort, L.; Bearpark, M. J.; Robb, M. A. *J. Phys. Chem. A* **2007**, *111*, 2182−2192.
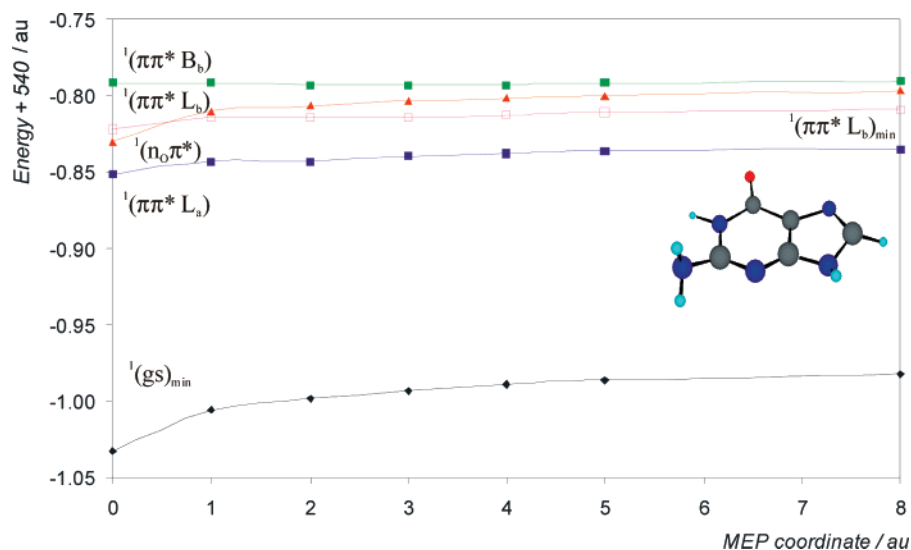
Figure 7. Low-lying singlet excited states of 9H-guanine computed at the CASPT2//CASSCF level from the Franck−Condon ground-state geometry along the minimum energy path (MEP) of the $^1(\pi\pi^*\ L_b)$ state.

Table 2. Computed Structures and Energy Differences for the Low-Lying Singlet Excited States of 9H-Guanine at the CASPT2// CASSCF(14,12)/6-31G(d, p) Level[a]

		energy differences (kcal mol^{-1})		
structure	description	ΔE_1[b]	ΔE_2[c]	ΔE_3[d]
(gs/$\pi\pi^*\ L_a$)$_{CI}$	CI ^{1}gs/$\pi\pi^*\ ^1L_a$		0.0[e]	0.7
(gs/$n_O\pi^*$)$_{CI}$	CI ^{1}gs/$^1n_O\pi^*$	0.0 [$^1(n_O\pi^*)$]	−6.0	8.1
$^1(n_O\pi^*)_{TS}$	TS $^1(n_O\pi^*)_{min}$ - (gs/$^1n_O\pi^*$)$_{CI}$	1.6 [$^1(n_O\pi^*)$]	−4.4	−
$(n_O\pi^*/\pi\pi^*\ L_a)_{CI}$	CI $n_O\pi^*/\pi\pi^*\ ^1L_a$	12.2 [$^1(n_O\pi^*)$]	6.2	−
$(\pi\pi^*\ L_b/n_O\pi^*)_{CI}$	CI $\pi\pi^*\ ^1L_b/n_O\pi^*$	0.7 [$^1(\pi\pi^*\ L_b)$]	31.2	4.0
$(\pi\pi^*\ L_b/\pi\pi^*\ L_a)_{CI}$	CI $\pi\pi^*\ ^1L_b/\pi\pi^*\ ^1L_a$	0.3 [$^1(\pi\pi^*\ L_b)$]	30.8	3.3

[a] Transition states (TS): CASPT2//CASSCF level. Conical intersections (CI): CASPT2 explorations. [b] Between the structure and the minimum of the mentioned state. [c] Between the structure and the reference (gs/$\pi\pi^*\ L_a$)$_{CI}$ energy. [d] Splitting at the CI (CASPT2 level). The average energy has been used as reference. [e] At this level the CI (end of the MEP) is placed adiabatically with respect to the ground state at 4.3 eV.
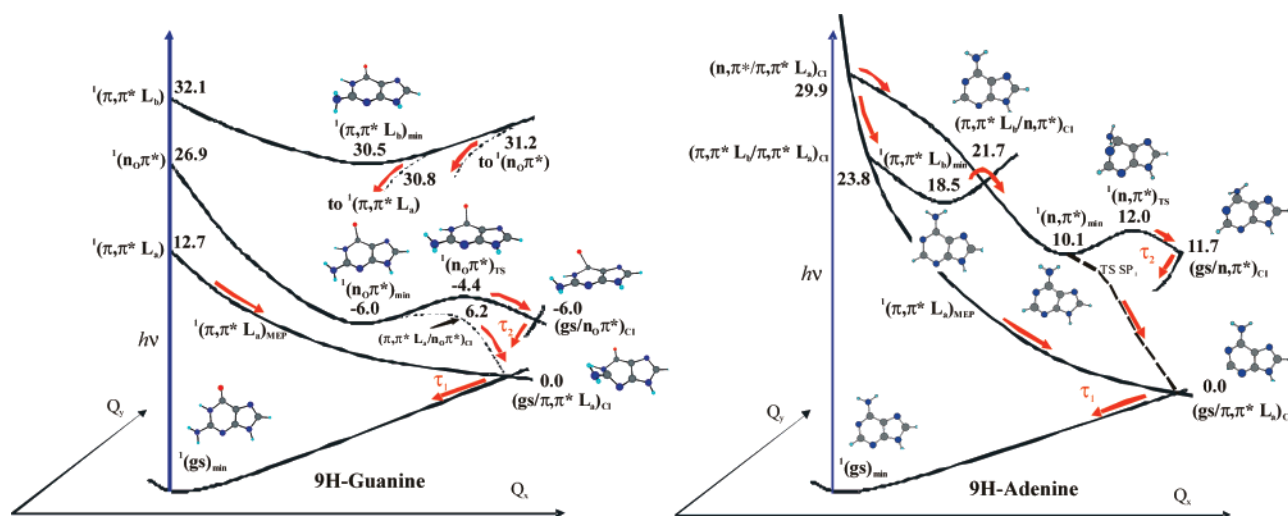

Figure 8. Scheme proposed, based on CASPT2 calculations, for the main decay pathways of 9H-guanine, measured in molecular beams with intrinsic lifetimes $\tau_1 < 148$ fs and $\tau_2 \approx 0.4$ ps.[10] An equivalent scheme for 9H-adenine has been included for comparison (see refs 17 and 24). In 9H-adenine the corresponding lifetimes are $\tau_1 < 100$ fs and $\tau_2 \approx 1.0$ ps.[10] Energies in kcal mol^{-1} referred to the lowest conical intersection (see also Table 2 and text).

As shown earlier,[56] another $n_N\pi^*$ singlet state lies too high in energy, and the main energy relaxation paths do not involve it. As a whole, these findings are used to interpret the nonadiabatic photochemistry of 9H-guanine on the basis of a three-state model, which is summarized in Figure 8, where a scheme of the photochemistry of 9H-adenine has also been included for the sake of comparison.

Guanine photophysics is very rich, whatever is in isolated conditions or in solvated environments or integrated in polynucleotide chains. We will start our discussion with the data measured in molecular beams. The most interesting features in the photophysics of the DNA/RNA nucleobases are the ultrashort radiationless decay times obtained both for jet-cooled or solvated species. Early experiments on base monomers in

aqueous solution (see a detailed review in ref 8) proved that S_1 lifetimes were small, well below the experimental time resolution at that time, typically 1 ps. The measured short decay times are consistent with the broad and diffuse bands observed in the molecular beam experiments.[8,10] The proposal that the band origin for the low-lying $\pi\pi^*$ state in 9H-guanine is absent in the gas-phase UV spectra[30] is totally consistent with the present results, which indicate a barrierless path toward an accessible CI and the absence of a local minimum along the main relaxation profile. Excited-state dynamics studies on isolated nucleobases were performed by measuring fluorescence lifetimes or by time-resolved pump−probe REMPI detection with different time resolutions. Kang et al.[75] reported the first pump−probe mass spectroscopy study with femtosecond pulses on the nucleobases at an excitation energy of 267 nm (4.64 eV), describing a single-exponential decay with averaged state lifetimes 1.0 ps for adenine, 0.8 ps for guanine, and larger values for the pyrimidine bases. More recently, Canuel et al.[10] employed highly resolved mass-selected femtosecond pump−probe transient resonant ionization (TRI) spectroscopy to investigate the decay mechanisms of all nucleobases and several methyl derivatives after excitation at 267 nm (4.64 eV). The measurements, performed with a high time resolution of 80 fs, provided a double exponential fitting leading to ultrafast, 148 fs, and intermediate, 0.36 ps, components for guanine, and similar values for the other nucleobases. All those data were interpreted by Canuel et al.[10] in terms of a two-state model: once the spectroscopic state was populated, the 148 fs step would correspond to the internal relaxation of the $^1(\pi\pi^*)$ state toward its minimum, followed by a slower step of 0.36 ps assigned to a switch to the $^1(n\pi^*)$ state and further relaxation to the ground state through a $(gs/n\pi^*)_{CI}$ CI, in which the C_6N_1 bond would be the protagonist. We try here to improve such a model in the light of our new results, shown also to be consistent with recent reports[76] on the presence in pyrimidine nucleobases in solution of a second deactivation path via a low-lying dark intermediate state attributed to the singlet $^1(n_O\pi^*)$ state, a channel whose relevance has still to be determined and whose presence does not necessarily question the mentioned photostability of nucleobases.

Considering together our computed results for 9H-adenine and 9H-guanine, we propose a similar photophysical scheme for the two molecules (see Figure 8) based on a three-state model. The cornerstone of their photochemistry is the repulsive nature of the bright $^1(\pi\pi^*\ L_a)$ state which relaxes in a barrierless manner from the FC region to a low-lying funnel connecting with the ground state, $(gs/\pi\pi^*\ L_a)_{CI}$. Taking into account that the $^1(\pi\pi^*\ L_a)$ state is involved in the most strongly allowed transition dominating the low-lying absorption spectrum, most of the energy acquired by illuminating the molecule will rapidly decay along its hypersurface to the ground state, quenching the fluorescence. Whether the ^1L_a state is the lowest excited singlet state (guanine) or not (adenine) at the FC region, in both cases it is clearly a bright spectroscopic state directly populated upon absorption at low energies, and able to relax in a barrierless way toward the ground state. The presence of a measured ultrashort lifetime between 100 and 148 fs in both systems[10]

can therefore be explained by a fast internal conversion to the ground state. We think that the ultrafast decay which is always recorded at energies higher than 267 nm should be better attributed to the $^1(\pi\pi^*\ L_a)$ state, which carries most of the population, rather than to the $^1(\pi\pi^*\ L_b)$ state. Additional 50 fs channels have been reported by Ullrich et al.[77] in adenine after excitation to 267 nm, that we previously[17,24] attributed to the energy relaxation from the less populated $^1(\pi\pi^*\ L_b)$ state toward its minimum. This alternative seems more plausible than the suggested assignment to the $^1(\pi\sigma^*)$ dissociative state, which correlates in the FC region with a higher-lying and weak Rydberg transition and at long distances with the hydrogen-abstracted radical, which requires surmounting larger energy barriers (estimated about 5.4−5.5 eV)[28] above the lowest channel described here, as proved for adenine[24] and guanine.[36] The required energies, the presence of decay mechanisms and times very similar to those of adenine in derivatives such as 9-methyladenine or N,N-dimethyladenine,[10] and the absence of kinetic isotope effects[78] indicate that the different N−H dissociation channels cannot be responsible for the ultrafast decays in isolated nucleobases at low energies. They should be better related to the $^1(\pi\pi^*)$ channels, although new calculations and experiments are required, especially to check the possibility of tunneling and isotope effects in the H-loss processes. At present, it can be concluded that the $^1(\pi\sigma^*)$ path is probably not related to the already measured ultrafast relaxation processes in adenine and guanine and their nucleosides and nucleotides, although it can be certainly related to other fast decay processes at higher energies and in base pairs.[79]

A second, longer-lived decay (360 fs to 1.1 ps) has been observed for the purine nucleobases in the 250 and 267 nm experiments. In Figure 8 we describe different possible decay paths related to the low-lying $^1(\pi\pi^*\ L_b)$ and $^1(n\pi^*)$ states to which this decay can be better attributed. In adenine[24] the $^1(\pi\pi^*\ L_b)$ and $^1(n\pi^*)$ states will be basically populated through the crossing with the $^1(\pi\pi^*\ L_a)$ PEH and, in a minor extent, by direct absorption, in particular the transition to $^1(\pi\pi^*\ L_b)$, carrying more intensity. The decay can therefore proceed from $^1(\pi\pi^*\ L_b)_{min}$ via a state switch to the $^1(n\pi^*)$ state, reaching its minimum (the lowest on S_1 PEH), and from there, several relaxation pathways are possible: first, following the N_1C_6 bond torsion coordinate (NH_2 perpendicular to the ring) and via the $^1(n\pi^*)_{TS}$ transition state through the CI $(gs/n\pi^*)_{CI}$, and second, involving the torsion of the C_2N_3 (pyramidalization of the ring) through the transition state $^1(n\pi^*)_{TS\ SP1}$ connecting $^1(n\pi^*)_{min}$ with the $^1(\pi\pi^*\ L_a)$ hypersurface. The preferred pathway will be reached after a subtle balance between the available excess vibrational energy and the barrier heights. In 9H-guanine the $^1(\pi\pi^*\ L_b)$ state lies high in energy, and its contribution to the relaxation dynamics can be only expected at high excitation energies, when after reaching the state minima, a population switch toward lower states can take place through the higher-lying $(\pi\pi^*\ L_a/\pi\pi^*\ L_b)_{CI}$ and $(n_O\pi^*/\pi\pi^*\ L_b)_{CI}$ CIs (see Figure 8). A more plausible relaxation path at low energies may proceed along the $^1(n_O\pi^*)$ state. Even if it is related to a forbidden transition, the transfer of part of the population of the

(75) Kang, H.; Lee, K. T.; Jung, B.; Ko, Y. J.; Kim, S. K. *J. Am. Chem. Soc.* **2002**, *124*, 12958−12959.

(76) Hare, P. M.; Crespo-Hernández, C. E.; Kohler, B. *Proc. Natl. Acad. Sci. U.S.A.* **2007**, *104*, 435.

(77) Ullrich, S.; Schultz, T.; Zgierski, M. Z.; Stolow, A. *J. Am. Chem. Soc.* **2004**, *126*, 2262−2263.

(78) Cohen, B.; Hare, P. M.; Kohler, B. *J. Am. Chem. Soc.* **2003**, *125*, 13594−13601.

(79) Sobolewski, A. L.; Domcke, W. *Phys. Chem. Chem. Phys.* **2004**, *6*, 2763−2771.
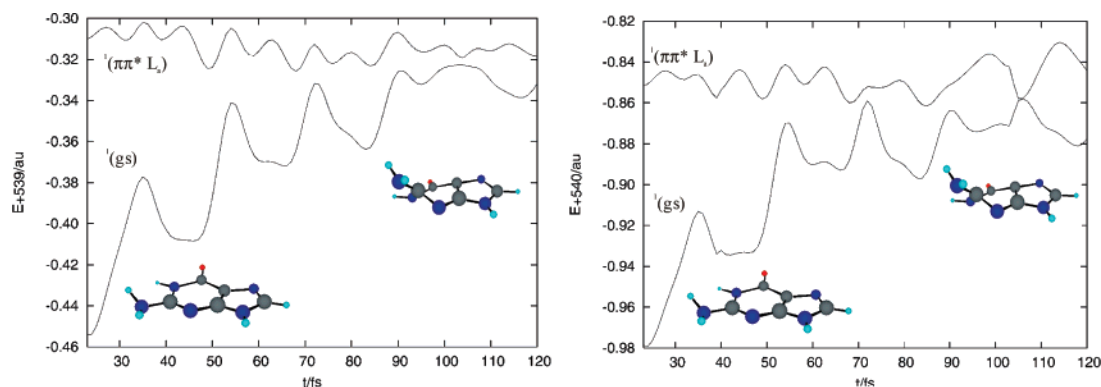
Figure 9. Sample classical trajectories run on the $^1(\pi\pi^* L_a)$ state of the 9H-guanine molecule starting at the FC geometry. On-the-fly computed CASSCF gradients and CASSCF (left) and CASPT2 (right) energies were employed. In these trajectories, the molecule reaches from the FC structure the $(gs/\pi\pi^* L_a)_{CI}$ region within the time period measured for the ultrafast decay, 148 fs.[10]

$^1(\pi\pi^* L_a)$ state upon excess vibrational energy is not unlikely, considering that the $^1(n_O\pi^*)$ minimum lies 6 kcal mol^{-1} lower than the $(gs/\pi\pi^* L_a)_{CI}$ at the end of the corresponding MEP. From that minimum the system may proceed toward the CI $(gs/n_O\pi^*)_{CI}$, placed isoenergetic with the minimum, surmounting the barrier computed to be 1.6 kcal mol^{-1} as the transition state $^1(n\pi^*)_{TS}$ (see Figure 8). Those structures (see Supporting Information) imply the torsion of the N_1C_6 bond and the oxygen atom becoming perpendicular to the ring, whose deformation corresponds to a puckered ^6E envelope structure, the same type of structure and profile found in the path toward the $(gs/n_N\pi^*)_{CI}$ CI in adenine.[17,24] This is not the only possibility. Once $^1(n_O\pi^*)_{min}$ has been reached, the relaxation may proceed via a CI $(\pi\pi^* L_a/n_O\pi^*)_{CI}$ toward the $^1(\pi\pi^* L_a)$ state PEHs, and finally to the funnel $(gs/\pi\pi^* L_a)_{CI}$. Similarly as in adenine, we propose the paths involving decays through $(gs/n_O\pi^*)_{CI}$ or switch $n_O\pi^*/\pi\pi^* L_a$ plus a decay through $(gs/\pi\pi^* L_a)_{CI}$ as the source of the 0.36 ps lifetime measured in guanine,[10] as we shall further discuss below.

Once the most favorable lowest-energy paths and associated barriers in the PEHs of the molecule are established, only actual calculations including time-dependent dynamic and statistic aspects shall be able to establish the accurate mechanistic details of guanine photodynamics and relate the reaction paths to the measured lifetimes. Here we will simply provide some illustration of those aspects in order to test qualitatively the previous attributes. Figure 9 contains two sample classical trajectories selected from a set and computed on the fly along the $^1(\pi\pi^* L_a)$ state PEHs starting from the FC geometry. They were obtained by using the velocity-Verlet algorithm[80] and employed ab initio two-state SA-CASSCF analytical gradients[81] in the full space of coordinates (see more details in the Supporting Information). In this two-state reaction dynamics calculations the molecule reaches, in a time period shorter than 148 fs, which is the measured lifetime for the ultrafast decay detected in guanine,[10] a region with a near degeneracy between the ground and the $^1(\pi\pi^* L_a)$ state and ends in a molecular structure close to $(gs/\pi\pi^* L_a)_{CI}$. These calculations, which have just a qualitative value, are part of a more complete and ongoing study of the molecule dynamics and help to illustrate that, as suggested also by us in other DNA/RNA nucleobases,[17,23–25,45] the system, at least along its low-energy paths, is able to reach the CI

$(gs/\pi\pi^* L_a)_{CI}$ within the measured <150 fs time period along a reduced number of trajectories. No time scale can be directly deduced so far, and certainly, a quantitative answer requires a more complete set of calculations.

On the other hand, recent studies on a modified aminopyrimidine model performed by Barbatti and Lischka[67] including also molecular dynamics calculations at the CASSCF/MRCI level and starting on a $\pi\pi^* L_b$-type state, obtained a near 1 ps decay for the reaction path which included transferring from $^1(\pi\pi^* L_b)$ to $^1(n_N\pi^*)$, reaching the minimum, and final progress toward the methanamine (CN)-like $(gs/\pi\pi^* L_a)_{CI}$ CI, with no evidence of NH$_2$ pyramidalization or crossing through $(gs/n_N\pi^*)_{CI}$. The role of the TS connecting the $^1(n\pi^*)$ and $^1(\pi\pi^* L_a)$ states becomes in that case important. Barbatti and Lischka's findings[67] perfectly agree with our previous proposals for adenine.[17,24] A similar scheme can be suggested for 9H-guanine, where the structures $^1(n_O\pi^*)_{min}$ and $(gs/n_O\pi^*)_{CI}$ become very favorable and below the first accessible $(gs/\pi\pi^* L_a)_{CI}$, although they are isoenergetic with the corresponding $(gs/\pi\pi^* L_a)_{MECI}$. A favorable decay path can be proposed to take place through the low-lying $^1(n_O\pi^*)$ minimum and toward the ground state via one of the two accessible CIs, $(gs/\pi\pi^* L_a)_{CI}$ and $(gs/n_O\pi^*)_{CI}$, and certainly it can be related to the measured 0.36 ps relaxation.[10] The presence of a low-energy $n\pi^*$ minimum has been already suggested in low-temperature solid-host experiments.[8] The present model does not require introducing an intersystem crossing mechanism to explain the observed decay processes.[77] More detailed simulations are in any case required. Regarding the measurements in aqueous solution at room temperature, guanine nucleoside and nucleotide yielded lifetimes of 0.46 and 0.86 ps, respectively.[7,82,83] Whereas it can be expected that the ultrafast (<150 fs) component may not have been measured in those conditions, it is more likely that the gas-phase 0.36 ps component[10] is related to that observed in solution, and probably larger because of the destabilization undergone by the $n\pi^*$ states in polar and protic environments.

3.4. Photochemistry of Nonnatural Guanine Tautomers. The same strategy employed to study the 9H-guanine photochemistry has been here used to analyze the properties of the singlet excited states of the most stable tautomers in the gas

(80) Andersen, H. C. *J. Comput. Phys.* **1983**, *52*, 24−34.
(81) Stålring, J.; Bernhardsson, A.; Lindh, R. *Mol. Phys.* **2001**, *99*, 103−114.

(82) Pecourt, J. M. L.; Peon, J.; Kohler, B. *J. Am. Chem. Soc.* **2000**, *122*, 9348−9349.
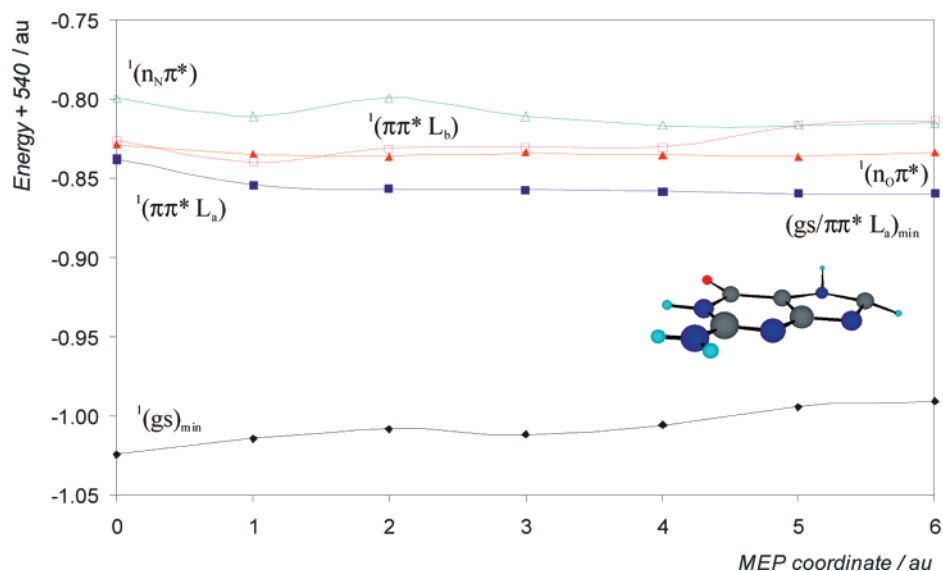(83) Pecourt, J. M. L.; Peon, J.; Kohler, B. *J. Am. Chem. Soc.* **2001**, *123*, 10370−10378.

Figure 10. Low-lying singlet excited states of 7H-guanine computed at the CASPT2//CASSCF level from the Franck−Condon ground-state geometry along the minimum energy path (MEP) on the $^1(\pi\pi^* \text{L}_a)$ state.

phase: 7H-guanine and two hydroxyl derivatives, 9H-6OH-guanine and 7H-6OH-guanine. Figure 10 (and Figures SI6−10 in the Supporting Information) display computed MEPs for the abovementioned molecules along their respective $^1(\pi\pi^* \text{L}_a)$ states' PEHs, whereas the corresponding MEPs along the $^1(\pi\pi^* \text{L}_b)$ states' PEHs have been collected in the Supporting Information. In all three cases the former state is related to the transitions with the largest oscillator strengths at low energies. The most striking feature is evidently the fact that all computed MEPs lead toward planar local minima, unlike what occurred in 9H-guanine, in which the $^1(\pi\pi^* \text{L}_a)$ MEP yields a barrierless path toward $(gs/\pi\pi^* \text{L}_a)_{CI}$. This behavior of guanine is not exclusive; also in adenine our previous studies proved that only in the natural tautomer the $^1(\pi\pi^* \text{L}_a)$ MEP is barrierless, and no local minima lie along the path unlike, for instance, in the similar species 7H-adenine and 2-aminopurine.[17,24] As the presence of the barrierless path can be associated with the existence of favorable and ultrafast internal conversion processes in the studied sytems, this common behavior can be envisaged as a pattern for natural nucleobases. They could be considered as the best outcome of natural selection to obtain those pieces for the genetic material that could become more stable upon UV irradiation, especially abundant in early stages of life on Earth.[8]

The presence of local minima along the MEPs, and consequently the existence of energy barriers decreasing the efficiency of the ultrafast decay, does not imply that a low-lying CI of the $(gs/\pi\pi^* \text{L}_a)_{CI}$ type does not exist. Such a crossing can be considered an intrinsic property of the system: it is related with the orbital structure in the molecule, H and L in particular, and derives from the fact that a biradical form can most probably be found at low energies. However, even if such funnels exist, higher barriers and longer, most favorable paths to access the corresponding CIs are computed in nonnatural nucleobases. In fact, as compiled in Table 2, we have computed similar $(gs/\pi\pi^* \text{L}_a)_{MECI}$ structures in all four guanine tautomers (see structures in the Supporting Information). They usually lie much lower in energies than any other state minima, but their photochemical relevance in 7H-guanine, 9H-6OH-guanine, and 7H-6OH-guanine should be considered minor, because an

energy barrier prevents favorable access to such CI seams. As proved before,[24] after surmounting the barrier related to the planar minima, there is a path leading to such CIs at low energies, but it will be difficult to obtain experimental evidence of its presence because of the extremely fast decay that would take place. In general, exciting at low energies leads to large lifetimes, sometimes in the order of nanoseconds, because true state minima are being populated, something that does not occur when the system evolves directly to the CI involving the bright $^1(\pi\pi^* \text{L}_a)$ state, which is a protagonist of the ultrafast relaxation by proper molecular deformations. Finally, it can be mentioned that optimization of the lowest $^1(n_N\pi^*)$ state in 9H-6OH-guanine directly leads to a CI with the ground state, $(gs/n_N\pi^*)_{CI}$ (see Supporting Information).

Controversy still remains about the role that the different mechanisms play into the deactivation of the nucleobases, although most of efforts have been concentrated on adenine and derivatives. Direct deactivation via the $\pi\pi^*$ state has been disputed on the basis that more amplitude in the transient spectrum of $n\pi^*$ has been detected at higher energies.[84] Such an argument ignores that two different $\pi\pi^*$ states are involved and nothing prevents an increased population of $n\pi^*$ through the L_b state, which is a relaxation process also suggested here as source of the picosecond decay in nucleobases. Also the proposed major participation of the in-plane N−H dissociation channel via a CI of the ground state and an $n\sigma^*$ state[31,32,77,84] is under debate,[17,24] and it has been recently questioned.[85,86] Most of the suggestions should have to wait until more comprehensive experiments and theoretical calculations including dynamics aspects are carried out at appropriate levels for all nucleobases and their nucleosides and nucleotides. A recent study[87] proved that upon a covalent substitution, for instance that in propanodeoxyguanosine, which consists of an additional ring that hinders the out-of-plane distortion of the six-membered guanine

(84) Satzger, H.; Townsend, D.; Zgierski, M. Z.; Patchkovskii, S.; Ullrich, S.; Stolow, A. *Proc. Natl. Acad. Sci. U.S.A.* **2006**, *103*, 10196−10201.
(85) Schneider, M.; Maksimenka, R.; Buback, F. J.; Kitsopoulos, T.; Lago, L. R.; Fischer, I. *Phys. Chem. Chem. Phys.* **2006**, *8*, 3017−3021.
(86) Nix, M. G. D.; Devine, A. L.; Cronin, B.; Ashfold, M. N. R. *J. Chem. Phys.* **2007**, *126*, 124312.
(87) Zgierski, M. Z.; Patchkovskii, S.; Takashige, F.; Lim, E. C. *Chem. Phys. Lett.* **2007**, *440*, 145−149.

ring, the ultrafast relaxation vanishes, in a fashion similar to that which happened when substituting adenine with an amino group in position C_2, yielding 2-aminopurine, a highly fluorescent purine derivative.[17]

IV. Summary and Conclusions

The photoinduced relaxation processes taking place in the guanine monomer have been studied by means of the high-quality ab initio multiconfigurational CASSCF/CASPT2 procedure. The potential energy hypersurfaces (PEHs) of the most stable tautomers of guanine have been mapped, looking for minima, transition states, conical intersections (CIs), and minimum energy paths (MEPs) in order to determine the lowest-energy relaxation paths after UV absorption. The present findings complement previous studies on the other natural DNA/RNA base monomers and allow designing a common framework to rationalize the measured multiexponential ultrafast decays detected in the molecules in the femtosecond and picosecond time range.[8,10,77] The strongest point of the present study is the calculation of MEPs describing the lowest-energy and most favorable reaction profiles, which lead to the accurate determination of energy barriers. In the natural 9H-guanine tautomer, once the bright $\pi\pi^*$ L_a HOMO → LUMO singlet excited state has been populated, the computed MEP leads the molecule in a barrierless way toward an out-of-plane methanamine (CN)-like CI. Its structure is of biradical type and connects the initially excited and the respective ground state, involving, in particular, the twisting of the C_2N_3 bond and the ring puckering of the ^{2}E-type envelope, denoted by (gs/$\pi\pi^*$ L_a)$_{CI}$. As suggested by sample classical trajectories reported here and computed using an ab initio on-the-fly procedure, the barrierless path can be related to the ultrafast femtosecond decay measured in molecular beams at 148 fs,[10] a feature common in the five natural nucleobases, which also display barrierless paths along the $\pi\pi^*$ HOMO → LUMO MEP. Interestingly, computed MEPs for the $\pi\pi^*$ L_a states in other nonnatural tautomers such as 7H-guanine, 9H-6OH-guanine, and 7H-6OH-guanine lead directly to local planar minima, what indicates that an energy barrier is present along the decay, perturbing the ultrafast decay. This trend has been also obtained for other nonnatural nucleobase tautomers, for instance 7H-adenine and 2-aminopurine,[17,24] and points to the optimal natural selection of photostable monomers made by Nature. Other paths in guanine have been identified, in particular that involving a switch between the lowest-lying $^1(n_O\pi^*)$ minimum and leading to two possible decays: first, and after surmounting a few kcal mol^{-1} barrier represented by a transition state $^1(n_O\pi^*)_{TS}$, the system can reach the CI (gs/$n_O\pi^*)_{CI}$, in which the C_6N_1 bond twists and the six-membered ring distorts, undergoing an ^{6}E envelope pucker-

ing, with the oxygen atom almost perpendicular to the ring; second, and via the corresponding CI, the system can reach the $^1(\pi\pi^*$ L_a) state surface and the easily accessible (gs/$\pi\pi^*$ L_a)$_{CI}$. Either of these paths could be related to the measured 0.8–0.36 ps relaxation in molecular beams.[10,75] Finally, we have carried out a detailed study of the (gs/$\pi\pi^*$ L_a) CI seam. Different structures are found: at the end of the MEP we obtain (gs/$\pi\pi^*$ L_a)$_{CI}$, and by searching a minimum energy CI we obtain (gs/$\pi\pi^*$ L_a)$_{MECI}$. Mapping the seam of CIs shows that an energy barrier connects both structures, differing in particular in the dihedral angle related to the NH_2 amino group. Such a barrier is photochemically irrelevant because the system does not ride the seam of CIs; it will simply decay toward the ground state when reaching (gs/$\pi\pi^*$ L_a)$_{CI}$ in the first accessed region, that is, at the end of the MEP. The latter CI is therefore the one relevant in the photochemistry of guanine, unlike the (gs/$\pi\pi^*$ L_a)$_{MECI}$. Such findings enhance the importance of computing MEPs as a strategy to locate the really relevant CIs. On the basis of the present and similar quantum chemical studies, work in the future will have to be focused in two directions: a more accurate theoretical determination of the molecular properties in solution,[38,88–90] still today an unsolved task, and more extensive calculations including the dynamical aspects of the problem.

Supporting Information Available: Computational details, scheme with IUPAC's six-membered rings puckering nomenclature, shapes of relevant 9H-guanine CASSCF molecular orbitals, Cartesian coordinates of the optimized structures and absolute energies, minimum energy paths, linear interpolation in internal coordinates, several drawings of relevant molecular structrures: (gs/$\pi\pi^*$ L_a)$_{MECI}$ in all tautomers, several minima and CIs of 9H-guanine, and (gs/$n_N\pi^*)_{CI}$ in 9H-6OH-guanine, and, finally, complete refs 57 and 60 (supplied as refs 6 and 7, respectively). This material is available free of charge via the Internet at http://pubs.acs.org.

JA0744450

(88) Yamazaki, S.; Kato, S. *J. Am. Chem. Soc.* **2007**, *129*, 2901–2909.
(89) Ritze, H.-H.; Lippert, H.; Samoylova, E.; Smith, V. R.; Hertel, I. V.; Radloff, W.; Schultz, T. *J. Chem. Phys.* **2005**, *122*, 224320.
(90) Mennucci, B.; Toniolo, A.; Tomasi, J. *J. Phys. Chem. A* **2001**, *105*, 4749–4757.